iScience

CellPress
OPEN ACCESS

Article

Neurogenetic identification of mosquito sensory neurons

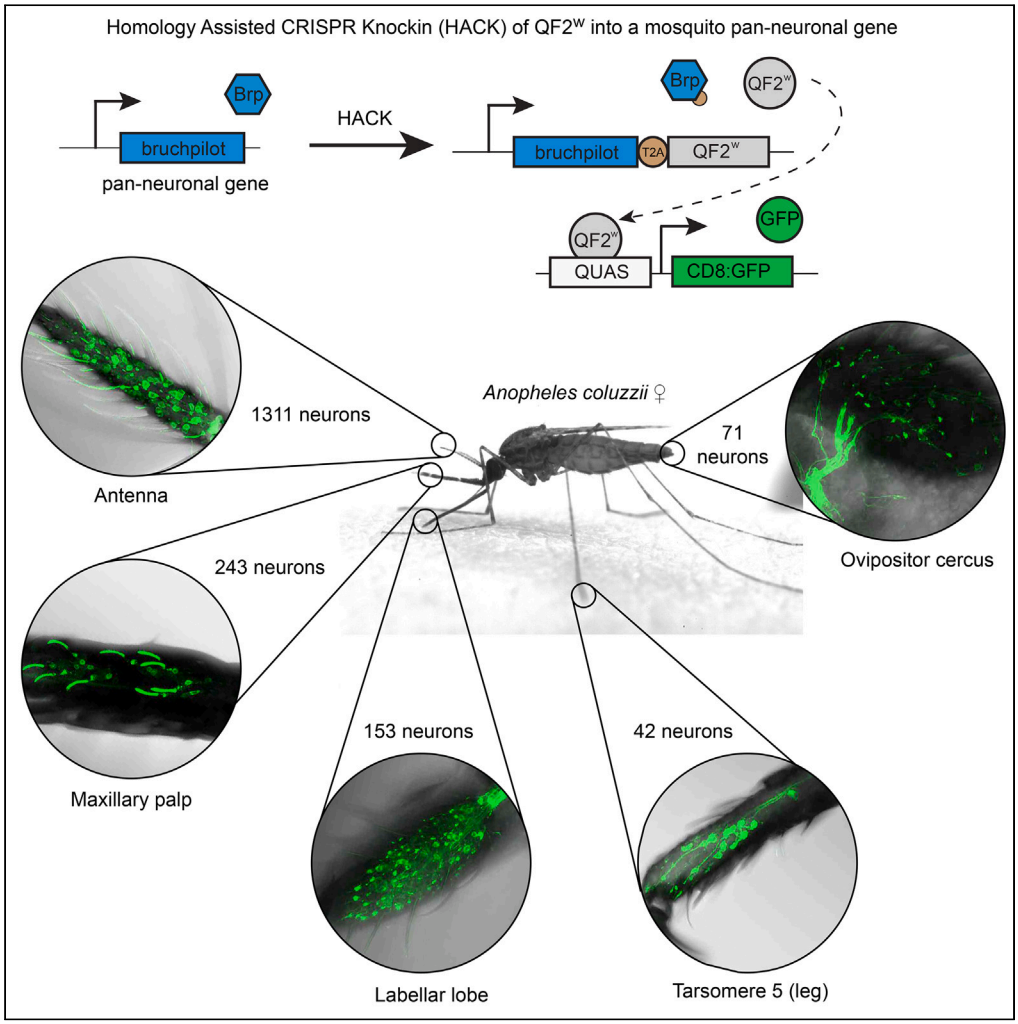

Joanna K. Konopka, Darya Task, Danny Poinapen, Christopher J. Potter

cpotter@jhmi.edu

Highlights

An efficient CRISPR/Cas9-based knock-in method for mosquitoes is described

A pan-neuronal labeling method for *Anopheles coluzzii* mosquitoes is introduced

All neurons in female mosquito sensory appendages are identified and quantified

Anopheles mosquitoes contain ~3,400 neurons in their sensory head appendages

Konopka et al., iScience *26*, 106690
May 19, 2023
https://doi.org/10.1016/j.isci.2023.106690

iScience

CellPress
OPEN ACCESS

Article

Neurogenetic identification of mosquito sensory neurons

Joanna K. Konopka,[1] Darya Task,[1,3] Danny Poinapen,[2] and Christopher J. Potter[1,4,*]

SUMMARY

***Anopheles* mosquitoes, as vectors for the malaria parasite, are a global threat to human health. To find and bite a human, they utilize neurons within their sensory appendages. However, the identity and quantification of sensory appendage neurons are lacking. Here we use a neurogenetic approach to label all neurons in *Anopheles coluzzii* mosquitoes. We utilize the homology assisted CRISPR knock-in (HACK) approach to generate a *T2A-QF2^{w}* knock-in of the synaptic gene *bruchpilot*. We use a membrane-targeted GFP reporter to visualize the neurons in the brain and to quantify neurons in all major chemosensory appendages (antenna, maxillary palp, labella, tarsi, and ovipositor). By comparing labeling of brp>GFP and Orco>GFP mosquitoes, we predict the extent of neurons expressing ionotropic receptors (IRs) or other chemosensory receptors. This work introduces a valuable genetic tool for the functional analysis of *Anopheles* mosquito neurobiology and initiates characterization of the sensory neurons that guide mosquito behavior.**

INTRODUCTION

Female mosquitoes are a threat to global human health as they can transmit various diseases through their bites. The *Anopheles* species of mosquitoes are the deadliest animals on earth as many prefer to bite humans and can serve as vectors of malaria, which kills ~600,000 people each year.[1] Female anthropophilic mosquitoes rely heavily on their finely tuned sensory systems to forage, mate, locate human hosts, and select oviposition sites.[2] These major behavioral decisions affecting their survival and fitness utilize mechanical (including sound reception), visual, and olfactory cues.[2–7] Olfaction is one of the most critical sensory modalities, involved in many mosquito behaviors, and plays a major role in host seeking.[6–9]

Mosquito behaviors occur in response to stimuli being detected by neurons in sensory appendages, and this information being transmitted, processed, and integrated in the brain. The main mosquito chemosensory appendages involved in host searching and bite site location include antennae, maxillary palps, and the labella of the mouthpart (Figures 1A and 1B). Sensilla (specialized hairs) on the surface of these sensory appendages house neurons. Dendrites of those neurons express receptors that interact with chemosensory cues in the environment. Various combinations of these chemosensory receptors allow for detection and discrimination of a vast number of odorants and other environmental cues, ultimately guiding females in their behaviors. The largest gene families of receptors involved in olfaction are odorant receptors (ORs), ionotropic receptors (IRs), and gustatory receptors (GRs). Current research focuses on the functional analysis of these receptors and creation of mutant mosquitoes targeting individual subunits or chemosensory co-receptors in order to determine their role in mosquito host-searching behavior.[10–20]

Advancements in genetic engineering have led to development of new tools and technologies, now routinely used in insect model and non-model organisms. Among those tools are CRISPR/Cas9,[21] the Q-system of binary expression,[22–24] and homology assisted CRISPR knock-in (HACK).[25] These tools have enabled the creation of *Drosophila* and mosquito lines with new transgenes and targeted mutations (both knock-in and knock-out), shedding light on the neuronal bases of insect chemosensory-guided behaviors.[10,13,19,25,26] Yet, genetic reagents that target individual mosquito chemoreceptor genes provide only a glimpse of the complexity of the mosquito chemosensory system. As such, the position, number, and identity of the complement of neurons within the chemosensory appendages of a mosquito are

[1]The Solomon H. Snyder Department of Neuroscience, Johns Hopkins University School of Medicine, Baltimore, MD, USA

[2]Robarts Research Institute, Schulich School of Medicine and Dentistry, Western University, London, ON, Canada

[3]Present address: Department of Biology, Johns Hopkins University, Baltimore, MD, USA

[4]Lead contact

*Correspondence: cpotter@jhmi.edu

https://doi.org/10.1016/j.isci.2023.106690

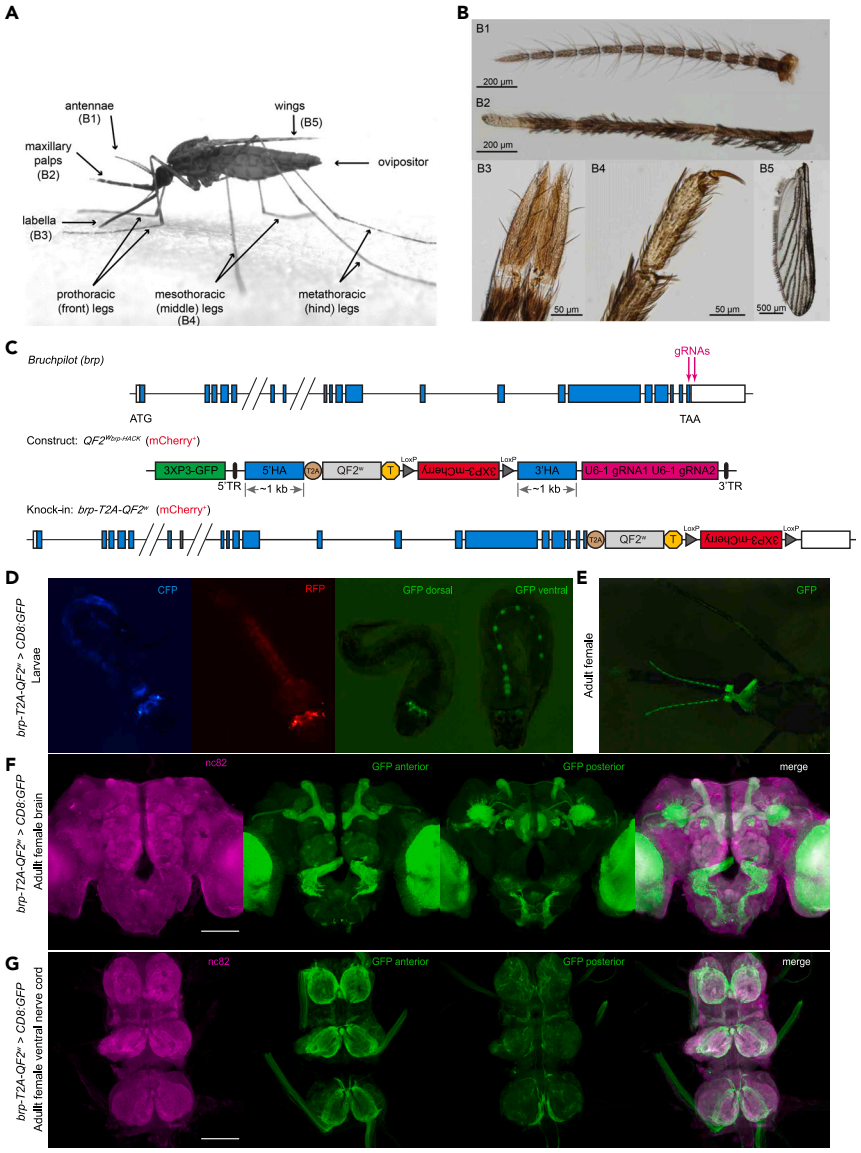

Figure 1. Generation and validation of *brp-T2A-QF2^{w}* HACK knock-in driver line for pan-neuronal expression in *Anopheles coluzzii* mosquitoes

(A) *An. coluzzii* female mosquito with chemosensory appendages highlighted.

(B) Chemosensory appendages of the head and the body.

(C) Schematic diagram of HACK knock-in strategy. Top: *An. coluzzii bruchpilot* (*brp*) target gene with exons indicated as blue boxes and introns as horizontal lines. Diagonal lines indicate truncation of long introns for visualization purposes. Guide RNAs (gRNAs) targeting the stop codon of *brp* gene are indicated by pink vertical arrows. Middle: *QF2w$^{brp\text{-}HACK}$* construct with gRNAs (pink), *T2A-QF2^{w}* (tan and gray, respectively), floxed *3XP3-mCherry* eye marker (red), and transcriptional stop (T; yellow). TR, piggyBac terminal repeat. Additional *3XP3-GFP* (green) was added upstream of the 5′ homology arm (5′HA; blue) to allow screening against random insertions of the construct in the genome. Bottom: The final knock-in *brp-T2A-QF2^{w}* with the construct integrated at the end of *brp* gene. The knock-in can be crossed to a reporter (*QUAS-CD8:GFP*) to examine the endogenous expression pattern of the *brp* gene (D) *brp-T2A-QF2^{w}* > *QUAS-CD8:GFP* larvae viewed under CFP (cyan fluorescent protein eye marker for *QUAS-CD8:GFP*), RFP (red fluorescent protein eye marker *for brp-T2A-QF2^{w}*), and GFP filters. GFP fluorescence indicates expression of *QUAS-CD8:GFP* in the brain and ventral nerve cord in the pattern of *brp* gene.

(E) *brp-T2A-QF2^{w}* > *QUAS-CD8:GFP* adult female with GFP fluorescence in the antennae and brain (visible through the cuticle).

Figure 1. *Continued*

(F) Maximum intensity projections of dissected brains of *brp-T2A-QF2^{w}* > *QUAS-CD8:GFP* females showing high levels of expression in the entire brain, including antennal lobe glomeruli and higher brain centers (n = 8). Endogenous GFP projections are separated into anterior (slices 1–22) and posterior (slices 23–50) views.

(G) Maximum intensity projections of dissected ventral nerve cords (VNC) of *brp-T2A-QF2^{w}* > *QUAS-CD8:GFP* females showing high levels of expression in all neuromeres (n = 6). Endogenous GFP projections are separated into anterior (slices 1–12) and posterior (slices 13–49) views. nc82 and merged channels in (F) and (G) are projections of full z stacks. Scale bars = 100 μm. See also Figure S1.

unknown. To address this limitation, a pan-neuronal line of *Aedes aegypti* mosquitoes was generated, allowing direct genetic access to all neurons in this species.[27] A similar pan-neuronal genetic reagent in *Anopheles* mosquitoes does not exist. The creation of genetic reagents in *Anopheles* mosquitoes, even in comparison to other non-model organisms like *Ae. aegypti* mosquitoes, is challenging and limited primarily due to low genetic transformation efficiency and survival. Nonetheless, a pan-neuronal *Anopheles* line could provide a roadmap to the number and spatial distribution of neurons within different sensory appendages. Additionally, having access to all neurons would allow the identification of new chemosensory gene targets and global functional analysis of chemosensory neuron responses to important odors, such as attractants and repellents.

Here, using the Q-system and HACK approach, we generate a pan-neuronal driver line for *Anopheles coluzzii* mosquitoes. We targeted the *bruchpilot* (*brp*) gene, which is involved in the structural integrity of neuronal presynaptic active zones. By inserting a *T2A-QF2^{w}* cassette before the stop codon of *brp*, we captured the expression pattern of Brp while maintaining its function. This *brp-T2A-QF2^{w}* pan-neuronal line enables genetic access to all neurons in the *Anopheles* mosquito. Utilizing a membrane-targeted green fluorescent protein (GFP) reporter line, we visualize, spatially map, and quantify neurons in different mosquito appendages. We focus predominantly on female chemosensory appendages relevant for host searching and biting. By comparing Orco and pan-neuronal populations, we quantify the likely full complement of IR neurons in the antenna. This study presents a comprehensive investigation of the neurons contained within the sensory appendages of the malaria mosquito.

RESULTS

Mosquitoes have several sensory appendages important for sensing their environment and executing behaviors (Figure 1A). The primary chemosensory appendages on a mosquito are the antenna, maxillary palp, and labella on the proboscis (Figure 1B). The wing margin (Figure 1B) may also contain chemosensory neurons.[28] Information about the full complement of neurons in an appendage could suggest the complexity or range of sensory responses by that appendage. For example, the total number of neurons in the mosquito antenna could indicate a maximum number of olfactory neurons in this tissue. However, the number of neurons that innervate *Anopheles* mosquito appendages is unknown. Neuronal stains could be used to identify neurons in an appendage, but this approach is time consuming, difficult to reproduce across many individuals, challenging to quantify, and could miss many neurons. The optimal approach would be to genetically label all neurons in the *Anopheles* mosquito by using a pan-neuronal driver line. When paired with a fluorescent reporter, such as GFP, this would robustly and reproducibly label all appendage neurons. We utilized such a genetic approach in this work to generate a comprehensive guide of neurons in an *Anopheles* mosquito's appendages.

Generation and validation of pan-neuronal driver line

To generate a pan-neuronal driver line in *An. coluzzii* mosquitoes, we used the Q-system of binary expression[24,29] paired with the "direct injection" approach of the HACK method.[25] We targeted the broadly expressed neural gene, *bruchpilot* (*brp*), which is involved in the structural integrity and function of neuronal synapses.[30–32] Antibodies to Bruchpilot are often used to label all neuropil in *Drosophila* and mosquito brains.[29,32] Recently, the *brp* gene was targeted to generate a pan-neuronal driver line in *Ae. aegypti* mosquitoes,[27] while the HACK approach was utilized to generate olfactory co-receptor knock-in lines in *Drosophila melanogaster*.[26] We targeted the last coding exon using two guide RNAs (gRNAs) to insert a *T2A-QF2^{w}* cassette with a *3xP3-mCherry* fluorescence eye selection marker before the stop codon of the *brp* gene (Figure 1C). The T2A is a self-cleaving peptide that induces ribosomal skipping, thus allowing two proteins to be produced from the same transcript; in this case a full-length brp protein (with a small T2A tag) that localizes to synapses and a functional QF2^{w} transcription factor

that enters the nucleus. By using this targeted knock-in approach, we captured the endogenous expression pattern of the *brp* gene without disrupting its normal function. The successful insertion of the HACK construct into the *An. coluzzii* genome was confirmed by PCR amplifying fragments spanning the *brp* gene with and without the knock-in constructs in wild-type and *brp-T2A-QF2^{w}* individuals (Figures S1A and S1B).

The *brp-T2A-QF2^{w}* individuals were crossed to the *QUAS-CD8:GFP* reporter line[29] to validate the pan-neuronal expression of the knock-in driver line. Endogenous GFP expression in the resulting progeny (*brp-T2A-QF2^{w}* > *QUAS-CD8:GFP*) was evident through the cuticle and easily observed in the brains and ventral nerve cords (VNCs) of larvae (Figure 1D) and various body regions of the adults (Figure 1E). We next used immunohistochemistry to examine brains (Figure 1F) and VNCs (Figure 1G) of *brp>CD8:GFP* adult females stained with antibody against Brp (nc82) to assess the overlap between the *brp-T2A-QF2^{w}* line and endogenous Brp expression. We observed broad GFP expression in the entire brain and VNC of the *brp>CD8:GFP* females, with the signal co-localized with anti-Brp staining. Major regions and structures of the brain were well labeled and distinguishable in the anterior (e.g., antennal lobes and glomeruli, mushroom bodies) and posterior (e.g., central complex, fan-shaped body, subesophageal zone) views (Figure 1F). A strong GFP signal was also observed in individual neuromeres of VNCs, which contain neurons relaying information to and from the brain, as well as motor and sensory neurons projecting to the rest of the body (Figure 1G). This broad brain and VNC labeling was consistent among individuals, and not observed in mosquitoes containing the *QUAS-CD8:GFP* reporter alone or in the *orco-T2A-QF2* > *QUAS-CD8:GFP* line (Figures S1C–S1F). These data suggest that the *brp-T2A-QF2^{w}* driver can serve as a robust pan-neuronal marker in *Anopheles* mosquitoes.

Quantification and characterization of *brp-T2A-QF2^{w}* expression in the sensory appendages of the mosquito head

We next characterized the labeling of the adult *brp>CD8:GFP* female peripheral nervous system, starting with the sensory appendages of the head (Figures 1A and 1B). We observed strong labeling of neuron cell bodies, nerve bundles, and dendritic projections into sensilla in antennae (Figure 2A), maxillary palps (Figure 2B), and labella (Figure 2C). We were also able to visualize the neurons of the labrum (the stylet used for blood feeding) extended out of the labium (the sheet housing the bundle of stylets) of the mouthpart (Figure 2D). These images allowed us to generate a comprehensive accounting of neurons in *Anopheles* chemosensory appendages.

While the endogenous GFP signal in the appendages of *brp>CD8:GFP* individuals was sufficient for visualization of neurons, the quantification of the total number of neurons in those appendages was challenging due to image contrast differences among very brightly and very dimly labeled cells, and the overlap of densely packed neurons in large datasets. To overcome these challenges and to count neurons more efficiently and consistently, we developed a semi-automatic pipeline for image pre- and post-processing to optimize 3-dimensional (3D) neuronal counting (Figure S2). The resulting processed images had enhanced contrast and masked any unwanted features that could interfere with counting (Video S1). The enhancement of the GFP signal in images processed with our pipeline enabled us to detect and count ~42% more neurons in individual antennal segments (n = 6) compared to manual counts of unprocessed images (data not shown).

Using our pipeline, we processed images of individual segments of antennae, maxillary palps, and labellar lobes of *brp>CD8:GFP* and *orco>CD8:GFP* female *An. coluzzii* and counted the neurons in those appendages. A single antenna of *brp>CD8:GFP* female mosquito contained an average of 1,311 ± 43 (mean ± SEM) neurons, 841 ± 23 (mean ± SEM) (64%) of which were Orco-positive (Orco+) (Figure 2E). Interestingly, the number of neurons was not distributed equally across the individual segments of the antenna (Figure 2G). Specifically, the total number of neurons increased from the proximal (closest to the head) to distal (the tip) segments of the antenna. This increase in number of neurons was not due to Orco+ neurons, since their numbers stayed mostly unchanged throughout the entire antenna, with the exception of the most distal and most proximal segments. While the identity of the Orco-negative antennal neurons is unknown, they most likely belong to neurons that express the IR olfactory receptor family, as reported by prior RNAseq studies[33] and recent *in situ* analysis.[34] Additionally, flagellomere 1 (the most proximal segment) contains only Orco-negative neurons, which likely include the ~22 Ir93a+ receptor neurons.[20]

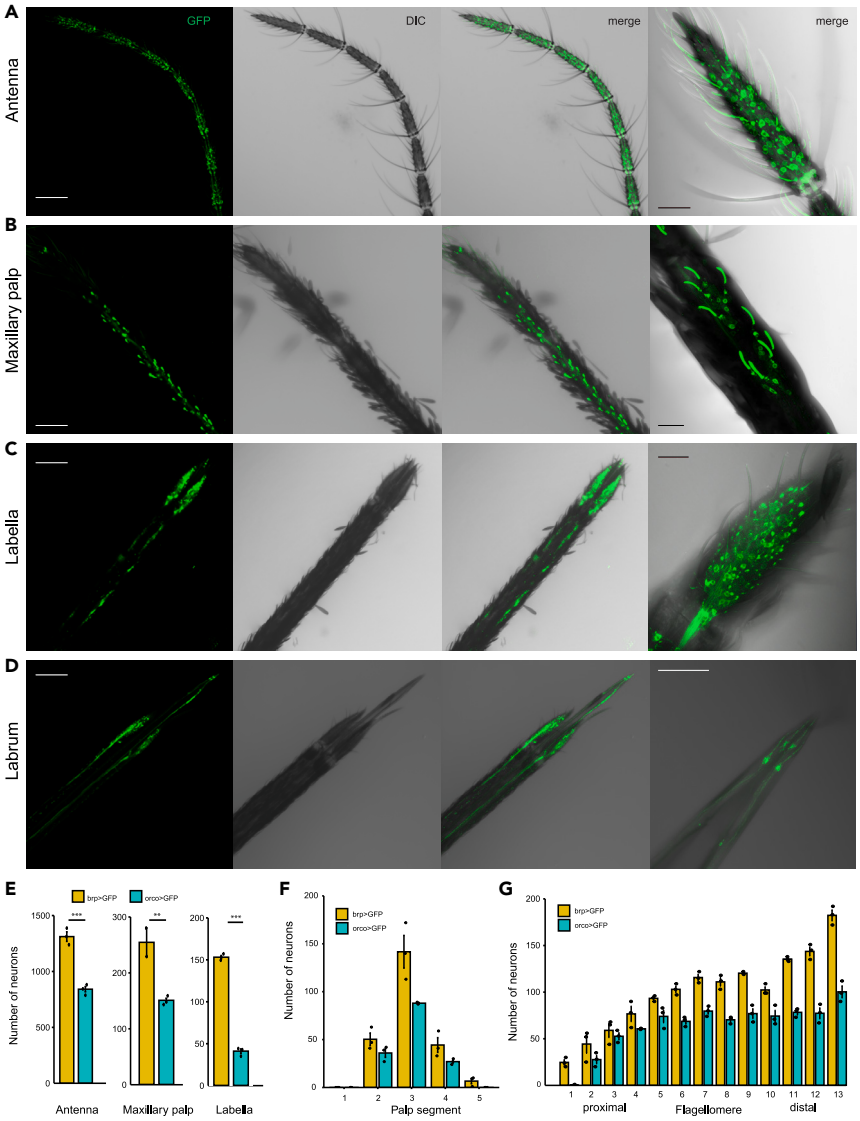

Figure 2. GFP expression in head sensory appendages of *brp-T2A-QF2^{w}* > *QUAS-CD8:GFP* female *An. coluzzii*

Maximum intensity projections of z stacks from (A) antennae, (B) maxillary palps, (C) proboscis with labella, and (D) labrum (blood-feeding stylet). Images on far right: higher magnification of (A) single antennal segment, (B) section of the maxillary palp, (C) tip of the proboscis (labella), and (D) tip of labrum. Images of individual appendages are obtained from different female mosquitoes.

(E) Mean ± SEM number of neurons in a whole antenna, whole maxillary palp, and labellar lobe (n = 3 for each genotype).

(F) Mean ± SEM number of neurons in individual segments of the maxillary palp (n = 3 for each segment of each genotype).

(G) Mean ± SEM number of neurons in individual flagellomere of the antenna (n = 3 for each segment of each genotype).

Genotypes of female mosquitoes: brp>GFP: *brp-T2A-QF2^{w}* > *QUAS-CD8:GFP*; orco>GFP: *Orco-T2A-QF2* > *QUAS-CD8:GFP*. Scale bars in A-D are 100 μm (first 3 panels) and 25 μm (far right panels). Statistical comparison in (E) based on independent samples t-test ($\alpha = 0.05$) ***$p < 0.001$, **$p < 0.01$, *$p < 0.5$.

A single female maxillary palp contained an average of 243 ± 23 (mean ± SEM) neurons, and a single female labellar lobe contained on average 153 ± 2 (mean ± SEM) neurons. Maxillary palps and labella of *brp>CD8:GFP* females also contain large populations of Orco-negative neurons (Figure 2E). These Orco-negative neurons account for approximately 38% and 73% of neurons in the maxillary palps and labella, respectively. We also observed neurons in the terminal (most distal) segment of the maxillary palps in the *brp>CD8:GFP* females but not in *orco>CD8:GFP* females (Figure 2F). The large number of Orco-negative neurons detected in the maxillary palp and labella most likely belong to neurons expressing IR and GR gene families.[33,35]

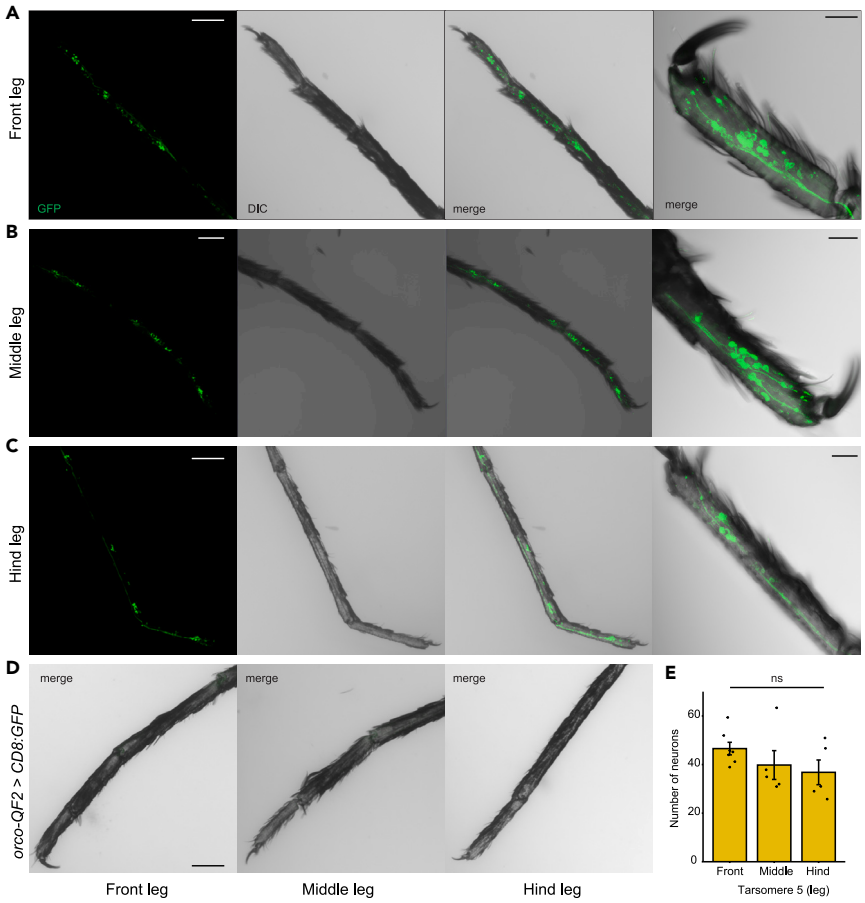

Figure 3. GFP expression in body sensory appendages of *brp-T2A-QF2^{w} > QUAS-CD8:GFP* female *An. coluzzii*

(A–C) Maximum intensity projections of z stacks from (A) front (prothoracic), (B) middle (mesothoracic), (C) hind (metathoracic) terminal tarsal leg segments of *brp-T2A-QF2^{w} > QUAS-CD8:GFP* female mosquitoes. Far right in (A–C): higher magnification images of fifth tarsal segment only.

(D) Maximum intensity projections of z stacks from front, middle, and hind terminal tarsal leg segments of *orco-T2A-QF2 > QUAS-CD8:GFP* female mosquitoes.

(E) Mean ± SEM number of neurons in fifth tarsomere of front (n = 7), middle (n = 5), and hind (n = 5) legs of *brp-T2A-QF2^{w} > QUAS-CD8:GFP* female mosquitoes. Statistical comparison based on 1-way ANOVA ($\alpha = 0.05$). Scale bars: 100 μm (first 3 panels in A-D) and 25 μm (far right panels in A–C).

Quantification and characterization of *brp-T2A-QF2^{w}* expression in the sensory appendages of the mosquito body

We also investigated the GFP expression in female sensory appendages that have not been well characterized (Figure 1A), including legs (Figures 3A–3C), wings, and the ovipositor (Figure 4). We found that prothoracic (front), mesothoracic (middle), and metathoracic (hind) legs of *brp>CD8:GFP* females contain a large number of neurons (Figures 3A–3C), but only in several of the tarsal segments (tarsomeres). We focused our investigation on terminal (most distal) tarsomere 5, as this segment likely provides important tactile and chemosensory information to the female during contact interactions with plant and animal hosts. Tarsomere 5 of each individual front, middle and hind leg contained on average ~42 neurons (Figure 3E), none of which were Orco+ (Figure 3D). We also observed labeling of nerve fibers and dendritic projections of some tarsal neurons extending into sensilla.

We further quantified the number of neurons in the cerci of female terminalia. Although this structure is not precisely homologous with the "ovipositor" of other insects, we refer to it here as "ovipositor" for simplicity. Most of the ovipositor surface and terminal abdominal segments of *brp>CD8:GFP* females were covered with neurons (Figures 4A and 4B), with each cerci containing 71 ± 3 (mean ± SEM) neurons

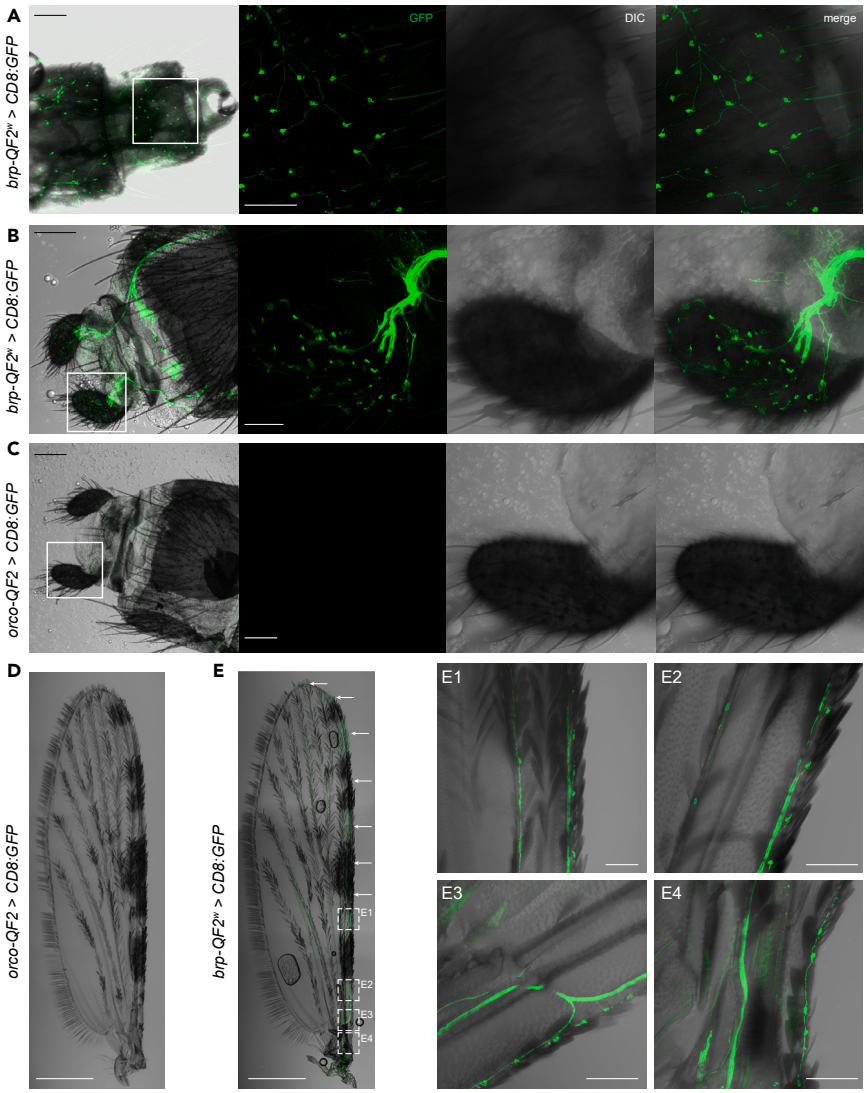

Figure 4. GFP expression in ovipositor and wings of *brp-T2A-QF2^{w} > QUAS-CD8:GFP* female *An. coluzzii*

(A) Maximum intensity projections of z stacks from last abdominal segments of *brp-T2A-QF2^{w} > QUAS-CD8:GFP* female mosquitoes. Cerci (on the terminal abdominal segment) of (B) *brp-T2A-QF2^{w} > QUAS-CD8:GFP* (n = 3) and (C) *orco-T2A-QF2 > QUAS-CD8:GFP* females (n = 3). Areas outlined with white boxes in (A-C) are magnified in panels to the right to show neuron cell bodies and their connections.

(D) Maximum intensity projection of z stacks (merged DIC and GFP channels) from a wing of *orco-T2A-QF2 > QUAS-CD8:GFP* female.

(E) Maximum intensity projection of z stacks (merged DIC and GFP channels) from a wing of *brp-T2A-QF2^{w} > QUAS-CD8:GFP* female mosquitoes. Higher magnification images of wing regions outlined with white dashed boxes are shown in E1-E4. Images in subpanels E1-E4 were not all obtained from the same wing and are used as representative images of the approximate areas indicated in (E). Neuron cell bodies were observed along the whole top wing margin beyond the areas marked in E1-E4 (indicated by white arrows). Images in D and E were stitched from serially acquired confocal images of the same wings obtained from either *orco-T2A-QF2 > QUAS-CD8:GFP* (D) or *brp-T2A-QF2^{w} > QUAS-CD8:GFP* (E) female mosquitoes. Scale bars for A-C: 100 μm (left most panels in A-C), 50 μm (zoomed in panels in A), 25 μm (zoomed in panels in B-C). Scale bars for D-E: 500 μm (D and E) and 50 μm (E1-E4).

(n = 3). Although we did not quantify the number of neurons in the wings, we observed innervation along the wing margins in *brp>CD8:GFP* females (Figure 4E). We did not find Orco+ neurons on wings or the ovipositor (Figures 4C and 4D). Taken together, our results identified the number of neurons in chemosensory appendages with implications on the chemosensory receptor families they may express.

DISCUSSION

We developed the first, to our knowledge, pan-neuronal driver line in *An. coluzzii* mosquitoes. By targeting the broadly expressed *bruchpilot* synapse gene, we have enabled genetic access to all neurons in *An. coluzzii* mosquitoes. We further demonstrated the utility of the HACK method, which combines a targeting cassette and gRNAs onto a single plasmid, as an efficient strategy of knocking-in constructs into the *Anopheles* mosquito genome. This approach might also increase knock-in efficiencies in other non-model organisms like *Ae. aegypti*. The pan-neuronal driver line utilizes the Q-system of binary expression and can be crossed to different Q-system compatible reporters for various applications to examine the structure and function of neurons in mosquitoes. Potential applications could include markers for the nucleus, RNAi constructs, calcium indicators, or stochastic labelers.

Prior RNAseq data suggest that female antennae predominantly contain ORs and IRs.[33] With only one GR (Gr1) enriched in female antennae,[33] the vast majority of the Orco-negative neurons we detected most likely express IRs. By comparing the number of neurons in *brp*>GFP and *orco*>GFP *An. coluzzii* female antennae, we can speculate on the distribution and abundance of IR-expressing neurons in the antennae. In contrast to $Orco^{+}$ antennal neurons whose numbers remain relatively constant from segment to segment, the number of the proposed IR^{+} neurons increases from proximal to distal antennal segments. This pattern of IR neuron number and distribution in the *An. coluzzii* antennae suggests that IR-expressing neurons are relatively enriched in distal flagellomeres, supporting fluorescent *in situ* hybridization data examining IR co-receptor expression pattens.[34] We also detected between 1 and 10 brp+ but Orco-negative neurons in proximal segment 1. These are likely the hygro- and thermo-sensory neurons that express Ir93a.[20]

The maxillary palps of *An. coluzzi* females also contain a mixture of Orco+ and Orco-neurons. This sensory appendage contains ~67 capitate peg sensilla, each housing 3 neurons: 1 GR+ and 2 Orco+.[33,36–38] These numbers predict a total of ~200 neurons innervating capitate peg sensilla across the entire maxillary palp. The mean number of neurons in maxillary palps of pan-neuronal females (*brp*>GFP) exceeded that number. With ~243 neurons total, there are an additional 43 neurons in each female palp that might not innervate capitate peg sensilla. Some of these neurons must be innervating campaniform sensilla and sensilla chaetica, which each contain a single mechanosensory neuron.[36] There is only 1 campaniform sensillum on maxillary palps of *An. gambiae* but likely numerous sensilla chaetica.[36,38] We are not aware of studies that quantified the number of sensilla chaetica on the maxillary palp of any *Anopheles* species, but the maxillary palps of *Ae. aegypti* contain 14 sensilla chaetica.[38] Since each campaniform sensilla and sensilla chaetica are innervated by a single neuron,[36] and if the number of sensilla chaetica are similar in number between *Aedes* and *Anopheles* mosquitoes, then we predict that at least 15 neurons would be represented by these types of sensilla in each *An. coluzzii* maxillary palp. This prediction suggests ~30 palpal neurons might possibly not be associated with known sensilla. Prior RNAseq analysis suggests that at least some of the neurons on the maxillary palps of *An. gambiae* express receptors belonging to the IR gene family.[33] These IRs might be expressed at low levels in GR+ and Orco+ neurons of the capitate pegs, as was reported for *Ae. aegypti*.[39] Additionally, IR + neurons could be among the additional ~30 cells not accounted for by known sensilla. Interestingly, there are no capitate peg sensilla on the most distal segment 5, but this segment does contain 1-10 brp+ neurons. Whether segment 5 neurons are mechanosensory or some are chemosensory remains to be determined.

Labella of *An. coluzzii* mosquitoes contain ~153 brp+ neurons per lobe, comprised of both Orco+ and Orco- neurons. These neurons innervate T1 and T2 sensilla, thought to be gustatory and olfactory, respectively.[35,38,40] There are ~30 T2 sensilla that contain ~60 olfactory neurons (2 neurons/T2 sensillum) per labellar lobe; by our analyses, only 41–45 of these are Orco+. This count suggests that up to 15 neurons in olfactory T2 sensilla might be expressing another family of olfactory receptors, such as IRs. In addition to ORs and IRs, labella also express many GR receptors.[19,35] These receptors are expressed on dendrites of neurons innervating large T1 gustatory sensilla. There are 15 gustatory sensilla per labellar lobe in *Ae. aegypti*[41] and *Ae. albopictus* (L. Baik; personal communication), while in *An. quadrimaculatus*, 28 total (14 per lobe) are reported.[42] By examining the labella of *An. coluzzii*, we counted 20-21 long hairs per labellar lobe, tapering towards the tip of the labella, which we presume are T1 sensilla. These sensilla match the locations of T1 sensilla used as stereotypic landmarks for T2 single sensillum recordings recordings.[35] Assuming the typical 5 neurons per gustatory sensillum (4 GR+ and one mechanosensory), there should be 105 neurons innervating T1 sensilla. Combined with the 60 olfactory sensilla, we can expect ~165 neurons in each labellar lobe. The total number of brp+ neurons (153) is below this predicted number (165), suggesting that there may be fewer than 5 neurons in some T1 sensilla.

Leg tarsi are the first appendages that come into direct contact with a plant or animal host. Since none of the neurons in the tarsi were Orco+, chemosensory neurons in *An. coluzzii* legs are likely IR+, GR+, or possibly TRP+ or ppk+.[43] The majority of sensory sensilla on the tarsi are predicted to be gustatory. Gustatory sensilla typically contain 4 GR+ chemosensory neurons and 1 mechanosensory neuron. Thus, the 42 neurons we observed on the 5th tarsomeres of front, middle, and hind legs might represent 8 gustatory sensilla with 32 chemosensory neurons that directly report on the taste of host skin, plant, or oviposition surfaces. Characterizing the taste profiles of these chemosensory neurons will be of great interest. Sensilla on leg tarsi may also represent targets for contact repellents such as N,N-diethyl-meta-toluamide (DEET). In *Ae. aegypti*, the contact repellency of DEET was *orco* independent[10] and required tarsal contact with a DEET treated surface.[44] Similarly, *An. coluzzii* females were not repelled by volatile DEET[45] but were repelled by DEET when it contacts their legs.[46] Thus, the 42 tarsal neurons identified here might contain receptor neurons that mediate aversion to DEET or other natural or synthetic repellents.

Our neurogenetic investigation allowed us to identify neurons in less studied and poorly understood sensory appendages of *An. coluzzii* female mosquitoes. Although we quantified the number of neurons in ovipositors but not the wings, both those sensory organs lacked Orco+ neurons suggesting they express other families of sensory receptors. Wings of *Drosophila melanogaster* contain gustatory receptors which respond to sweet and bitter stimuli and detect pheromones involved in courtship behavior.[28,47] Thus, the neurons in wings and ovipositors identified here for *An. coluzzii* might have sensory functions and play roles in mating or oviposition site selection.

We also noted interindividual variation in the number of neurons across different appendages. Among whole antennae from individual females, the number of neurons differed by 70-150 (*brp > CD8:GFP*) and by 24-80 for Orco+ neurons (*orco > CD8:GFP*), accounting for up to 11% difference in neuronal counts (see Limitations of the study). In palps and legs, the neuronal count among individuals differed by as much as 24% (62 neurons) and 76% (32 neurons), respectively. All else being equal (genetic background, imaging, image processing and neuron counting), this variation might reflect biological, rather than technical, differences. Phenotypic variation in traits is necessary for a population to have the ability to respond to natural selection and environmental changes.[48,49] In the mosquito chemosensory context, with appendages that are predominately required for taste and smell, this difference in number of neurons within individuals might translate into variation in the number of neurons expressing a particular chemoreceptor. For example, some individuals might have additional olfactory neurons expressing a receptor that responds to human-derived odors like decanal[50] or decanoic acid[13] and thus, confer to that individual higher sensitivity towards some human hosts. Conversely, additional neurons might instead express an OR more sensitive to "animal" odors,[50] making that individual more amenable to alternate blood-hosts. As such, individual females could have slightly different chemosensory sensitivities and behavioral responses in the context of the same chemical cues from attractants and repellents. Biological variability in chemosensory neuron numbers may afford individual mosquitoes in a population a range of response properties that promote survival and benefit the adaptability of the mosquito population as a whole. Future studies will be required to confirm the prevalence of interindividual differences in neuron numbers and if changes in sensory neuron numbers can influence individual behavioral preferences.

We successfully utilized the QF2 transcription factor to genetically target broad expression in the central and peripheral nervous system. The viability of the *brp-QF2^{w}* line suggests the Q-system can be an appropriate method to target any desired neuronal population in *Anopheles* mosquitoes. In this work, we targeted *T2A-QF2^{w}* before the stop codon of *bruchpilot* to allow full-length Bruchpilot to be expressed along with *QF2*. Similar approaches can be used to maintain the function of other genes while capturing their expression patterns. Alternatively, *T2A-QF2* (or just *QF2*) could be used to target near the start of the gene's coding region. This strategy would disrupt the function of the gene while still using the Q-system to capture its expression pattern.[34] This approach would be particularly useful to positively label the cells that contain the mutated gene.

The pan-neuronal line developed here opens up many new avenues of *Anopheles* mosquito research. For example, the pan-neuronal line along with a genetically encoded calcium indicator[51] enables identification of the neurons in the *Anopheles* mosquito that functionally respond to a variety of sensory stimuli, including various chemosensory attractants and repellents that influence host-seeking behaviors. Conversely, if further combined with an *orco* mutant,[11] it could be used to create a strain of *Anopheles* mosquitoes whose functional olfactory neurons were likely to be IR-expressing. This work represents an important step in the development of genetic tools for characterizing the biology of *Anopheles* mosquitoes.

Limitations of study

While we noted interindividual variation in the number of *brp>GFP* neurons, we did not determine if this translated to changes in the number of neurons expressing a particular chemosensory receptor. Thus, we can only hypothesize that interindividual differences in neuron numbers might be a neuronal mechanism to influence the transmission of sensory information from the periphery to the brain to drive behaviors. Additional studies using independent approaches, such as antibody staining for neuronal markers or electron microscopy reconstructions of appendages will be required to verify the presence of interindividual differences in appendage neuronal numbers.

The use of *brp-T2A-QF2*^{w} to drive robust expression of a calcium sensor (such as *QUAS-GCaMP6*) proved to be problematic in *Aedes aegypti* mosquitoes[27] prompting the investigators to utilize the stronger pan-neuronal synaptotagmin promoter to directly drive GCaMP6 expression. It is possible similar issues of inducing robust expression of a calcium sensor might exist in *Anopheles* mosquitoes, which would require the adoption of alternate approaches for pan-neuronal expression of calcium sensors.

STAR★METHODS

Detailed methods are provided in the online version of this paper and include the following:

- KEY RESOURCES TABLE
- RESOURCE AVAILABILITY
  - Lead contact
  - Materials availability
  - Data and code availability
- EXPERIMENTAL MODEL AND SUBJECT DETAILS
  - Mosquito rearing and colony maintenance
- METHOD DETAILS
  - Plasmid construction and HACK transgenesis
  - Construction of Anopheles coluzzii HACK backbone
  - Construction of AcoI QF2$^{brp-HACK}$ and QF2w$^{brp-HACK}$ plasmids
  - Knock-in line establishment and verification
  - Reporter expression
  - Life history and fitness of *brp-T2A-QF2*^{w} mosquitoes
- QUANTIFICATION AND STATISTICAL ANALYSIS

SUPPLEMENTAL INFORMATION

Supplemental information can be found online at https://doi.org/10.1016/j.isci.2023.106690.

ACKNOWLEDGMENTS

This work was supported by a Natural Sciences and Engineering Research Council of Canada Postdoctoral Fellowship to JKK and by grants from the National Institutes of Health (NIAID R01AI137078), the Department of Defense (W81XWH-18-1-0732), and the Johns Hopkins Malaria Research Institute (Pilot Fund) to CJP. We thank Barbara Smith (JHU Microscope Facility) and Michele Pucak (JHU Imaging Core Facility) for technical assistance and advice in image acquisition. We thank Chun-Chieh Lin for assistance in cloning and plasmid construction. We thank the Johns Hopkins Malaria Research Institute and Bloomberg Philanthropies for their support.

AUTHOR CONTRIBUTIONS

J.K.K. and C.J.P. conceived, designed, and interpreted all experiments. J.K.K. and D.T. designed the HACK construct and performed immunohistochemistry on brains and VNCs. J.K.K. generated and characterized the transgenic line. J.K.K. performed confocal imaging of all chemosensory appendages. D.P. developed the image processing pipeline and processed the imaging data. J.K.K. and D.P. performed neuronal counts. J.K.K. and C.J.P. wrote the manuscript with inputs from D.T. and D.P..

DECLARATION OF INTERESTS

The authors declare no competing interests.

INCLUSION AND DIVERSITY

We support inclusive, diverse, and equitable conduct of research.

Received: December 5, 2022
Revised: March 6, 2023
Accepted: April 13, 2023
Published: April 18, 2023

REFERENCES

1. World Health Organization (2021). World Malaria Report 2021 (World Health Organization).

2. Montell, C., and Zwiebel, L.J. (2016). Chapter ten - mosquito sensory systems. In Advances in Insect Physiology, A.S. Raikhel, ed. (Academic Press), pp. 293–328. https://doi.org/10.1016/bs.aiip.2016.04.007.

3. Andrés, M., Su, M.P., Albert, J., and Cator, L.J. (2020). Buzzkill: targeting the mosquito auditory system. Curr. Opin. Insect Sci. *40*, 11–17. https://doi.org/10.1016/j.cois.2020.04.003.

4. van Breugel, F., Riffell, J., Fairhall, A., and Dickinson, M.H. (2015). Mosquitoes use vision to associate odor plumes with thermal targets. Curr. Biol. *25*, 2123–2129. https://doi.org/10.1016/j.cub.2015.06.046.

5. Raji, J.I., and DeGennaro, M. (2017). Genetic analysis of mosquito detection of humans. Curr. Opin. Insect Sci. *20*, 34–38. https://doi.org/10.1016/j.cois.2017.03.003.

6. Bowen, M.F. (1991). The sensory physiology of host-seeking behavior in mosquitoes. Annu. Rev. Entomol. *36*, 139–158. https://doi.org/10.1146/annurev.en.36.010191.001035.

7. Konopka, J.K., Task, D., Afify, A., Raji, J., Deibel, K., Maguire, S., Lawrence, R., and Potter, C.J. (2021). Olfaction in *Anopheles* mosquitoes. Chem. Senses *46*, bjab021. https://doi.org/10.1093/chemse/bjab021.

8. Takken, W. (1991). The role of olfaction in host-seeking of mosquitoes: a review. Int. J. Trop. Insect Sci. *12*, 287–295. https://doi.org/10.1017/S1742758400020816.

9. Takken, W., and Knols, B.G. (1999). Odor-mediated behavior of Afrotropical malaria mosquitoes. Annu. Rev. Entomol. *44*, 131–157. https://doi.org/10.1146/annurev.ento.44.1.131.

10. DeGennaro, M., McBride, C.S., Seeholzer, L., Nakagawa, T., Dennis, E.J., Goldman, C., Jasinskiene, N., James, A.A., and Vosshall, L.B. (2013). Orco mutant mosquitoes lose strong preference for humans and are not repelled by volatile DEET. Nature *498*, 487–491. https://doi.org/10.1038/nature12206.

11. Sun, H., Liu, F., Ye, Z., Baker, A., and Zwiebel, L.J. (2020). Mutagenesis of the orco odorant receptor co-receptor impairs olfactory function in the malaria vector *Anopheles coluzzii*. Insect Biochem. Mol. Biol. *127*, 103497. https://doi.org/10.1016/j.ibmb.2020.103497.

12. Carey, A.F., Wang, G., Su, C.-Y., Zwiebel, L.J., and Carlson, J.R. (2010). Odorant reception in the malaria mosquito *Anopheles gambiae*. Nature *464*, 66–71. https://doi.org/10.1038/nature08834.

13. De Obaldia, M.E., Morita, T., Dedmon, L.C., Boehmler, D.J., Jiang, C.S., Zeledon, E.V., Cross, J.R., and Vosshall, L.B. (2022). Differential mosquito attraction to humans is associated with skin-derived carboxylic acid levels. Cell *185*, 4099–4116.e13. https://doi.org/10.1016/j.cell.2022.09.034.

14. Greppi, C., Laursen, W.J., Budelli, G., Chang, E.C., Daniels, A.M., van Giesen, L., Smidler, A.L., Catteruccia, F., and Garrity, P.A. (2020). Mosquito heat seeking is driven by an ancestral cooling receptor. Science *367*, 681–684. https://doi.org/10.1126/science.aay9847.

15. Jové, V., Gong, Z., Hol, F.J.H., Zhao, Z., Sorrells, T.R., Carroll, T.S., Prakash, M., McBride, C.S., and Vosshall, L.B. (2020). Sensory discrimination of blood and floral nectar by *Aedes aegypti* mosquitoes. Neuron *108*, 1163–1180.e12. https://doi.org/10.1016/j.neuron.2020.09.019.

16. Liu, F., Ye, Z., Baker, A., Sun, H., and Zwiebel, L.J. (2020). Gene editing reveals obligate and modulatory components of the CO_2 receptor complex in the malaria vector mosquito, *Anopheles coluzzii*. Insect Biochem. Mol. Biol. *127*, 103470. https://doi.org/10.1016/j.ibmb.2020.103470.

17. McBride, C.S., Baier, F., Omondi, A.B., Spitzer, S.A., Lutomiah, J., Sang, R., Ignell, R., and Vosshall, L.B. (2014). Evolution of mosquito preference for humans linked to an odorant receptor. Nature *515*, 222–227. https://doi.org/10.1038/nature13964.

18. Ye, Z., Liu, F., Ferguson, S.T., Baker, A., Pitts, R.J., and Zwiebel, L.J. (2021). Ammonium transporter AcAmt mutagenesis uncovers reproductive and physiological defects without impacting olfactory responses to ammonia in the malaria vector mosquito *Anopheles coluzzii*. Insect Biochem. Mol. Biol. *134*, 103578. https://doi.org/10.1016/j.ibmb.2021.103578.

19. Ye, Z., Liu, F., Sun, H., Ferguson, S.T., Baker, A., Ochieng, S.A., and Zwiebel, L.J. (2022). Discrete roles of Ir76b ionotropic coreceptor impact olfaction, blood feeding, and mating in the malaria vector mosquito *Anopheles coluzzii*. Proc. Natl. Acad. Sci. USA *119*, e2112385119. https://doi.org/10.1073/pnas.2112385119.

20. Laursen, W.J., Budelli, G., Tang, R., Chang, E.C., Busby, R., Shankar, S., Gerber, R., Greppi, C., Albuquerque, R., and Garrity, P.A. (2023). Humidity sensors that alert mosquitoes to nearby hosts and egg-laying sites. Neuron *111*, 874–887.e8. https://doi.org/10.1016/j.neuron.2022.12.025.

21. Kistler, K.E., Vosshall, L.B., and Matthews, B.J. (2015). Genome engineering with CRISPR-Cas9 in the mosquito Aedes aegypti. Cell Rep. *11*, 51–60. https://doi.org/10.1016/j.celrep.2015.03.009.

22. Potter, C.J., Tasic, B., Russler, E.V., Liang, L., and Luo, L. (2010). The Q system: a repressible binary system for transgene expression, lineage tracing, and mosaic analysis. Cell *141*, 536–548. https://doi.org/10.1016/j.cell.2010.02.025.

23. Riabinina, O., and Potter, C.J. (2016). The Q-system: a versatile expression system for *Drosophila*. Methods Mol. Biol. *1478*, 53–78. https://doi.org/10.1007/978-1-4939-6371-3_3.

24. Riabinina, O., Luginbuhl, D., Marr, E., Liu, S., Wu, M.N., Luo, L., and Potter, C.J. (2015). Improved and expanded Q-system reagents for genetic manipulations. Nat. Methods *12*, 219–222. https://doi.org/10.1038/nmeth.3250.

25. Lin, C.C., and Potter, C.J. (2016). Editing transgenic DNA components by inducible gene replacement in *Drosophila melanogaster*. Genetics *203*, 1613–1628. https://doi.org/10.1534/genetics.116.191783.

26. Task, D., Lin, C.-C., Vulpe, A., Afify, A., Ballou, S., Brbic, M., Schlegel, P., Raji, J., Jefferis, G., Li, H., et al. (2022). Chemoreceptor co-expression in *Drosophila melanogaster* olfactory neurons. Elife *11*, e72599. https://doi.org/10.7554/eLife.72599.

27. Zhao, Z., Tian, D., and McBride, C.S. (2021). Development of a pan-neuronal genetic driver in Aedes aegypti mosquitoes. Cell Rep. Methods *1*, 100042. https://doi.org/10.1016/j.crmeth.2021.100042.

28. Raad, H., Ferveur, J.-F., Ledger, N., Capovilla, M., and Robichon, A. (2016). Functional gustatory role of chemoreceptors in *Drosophila* wings. Cell Rep. *15*, 1442–1454. https://doi.org/10.1016/j.celrep.2016.04.040.

29. Riabinina, O., Task, D., Marr, E., Lin, C.-C., Alford, R., O'Brochta, D.A., and Potter, C.J. (2016). Organization of olfactory centres in the malaria mosquito *Anopheles gambiae*.

Nat. Commun. *7*, 13010. https://doi.org/10.1038/ncomms13010.

30. Kittel, R.J., Wichmann, C., Rasse, T.M., Fouquet, W., Schmidt, M., Schmid, A., Wagh, D.A., Pawlu, C., Kellner, R.R., Willig, K.I., et al. (2006). Bruchpilot promotes active zone assembly, Ca2+ channel clustering, and vesicle release. Science *312*, 1051–1054. https://doi.org/10.1126/science.1126308.

31. Südhof, T.C. (2012). The presynaptic active zone. Neuron *75*, 11–25. https://doi.org/10.1016/j.neuron.2012.06.012.

32. Wagh, D.A., Rasse, T.M., Asan, E., Hofbauer, A., Schwenkert, I., Dürrbeck, H., Buchner, S., Dabauvalle, M.C., Schmidt, M., Qin, G., et al. (2006). Bruchpilot, a protein with homology to ELKS/CAST, is required for structural integrity and function of synaptic active zones in Drosophila. Neuron *49*, 833–844. https://doi.org/10.1016/j.neuron.2006.02.008.

33. Pitts, R.J., Rinker, D.C., Jones, P.L., Rokas, A., and Zwiebel, L.J. (2011). Transcriptome profiling of chemosensory appendages in the malaria vector *Anopheles gambiae* reveals tissue- and sex-specific signatures of odor coding. BMC Genom. *12*, 271. https://doi.org/10.1186/1471-2164-12-271.

34. Raji, J.I., Konopka, J.K., and Potter, C.J. (2023). A spatial map of antennal-expressed ionotropic receptors in the malaria mosquito. Cell Rep. *42*, 112101. https://doi.org/10.1016/j.celrep.2023.112101.

35. Saveer, A.M., Pitts, R.J., Ferguson, S.T., and Zwiebel, L.J. (2018). Characterization of chemosensory responses on the labellum of the malaria vector mosquito, *Anopheles coluzzii*. Sci. Rep. *8*, 5656. https://doi.org/10.1038/s41598-018-23987-y.

36. McIver, S., and Siemicki, R. (1975). Palpal sensilla of selected anopheline mosquitoes. J. Parasitol. *61*, 535–538. https://doi.org/10.2307/3279338.

37. Lu, T., Qiu, Y.T., Wang, G., Kwon, J.Y., Rutzler, M., Kwon, H.-W., Pitts, R.J., van Loon, J.J.A., Takken, W., Carlson, J.R., and Zwiebel, L.J. (2007). Odor coding in the maxillary palp of the malaria vector mosquito *Anopheles gambiae*. Curr. Biol. *17*, 1533–1544. https://doi.org/10.1016/j.cub.2007.07.062.

38. McIver, S.B. (1982). Sensilla of mosquitoes (Diptera: Culicidae)1, 2. J. Med. Entomol. *19*, 489–535. https://doi.org/10.1093/jmedent/19.5.489.

39. Herre, M., Goldman, O.V., Lu, T.-C., Caballero-Vidal, G., Qi, Y., Gilbert, Z.N., Gong, Z., Morita, T., Rahiel, S., Ghaninia, M., et al. (2022). Non-canonical odor coding in the mosquito. Cell *185*, 3104–3123.e28. https://doi.org/10.1016/j.cell.2022.07.024.

40. Kwon, H.-W., Lu, T., Rützler, M., and Zwiebel, L.J. (2006). Olfactory responses in a gustatory organ of the malaria vector mosquito *Anopheles gambiae*. Proc. Natl. Acad. Sci. USA *103*, 13526–13531. https://doi.org/10.1073/pnas.0601107103.

41. Hill, S.R., and Berry Smith, J.J. (1999). Consistent pattern in the placement of taste sensilla on the labellar lobes of *Aedes aegypti*. Int. J. Insect Morphol. Embryol. *28*, 281–290. https://doi.org/10.1016/S0020-7322(99)00031-8.

42. Sparks, J.T., and Dickens, J.C. (2016). Electrophysiological responses of gustatory receptor neurons on the labella of the common malaria mosquito, *Anopheles quadrimaculatus* (Diptera: Culicidae). J. Med. Entomol. *53*, 1148–1155. https://doi.org/10.1093/jme/tjw073.

43. Baik, L.S., and Carlson, J.R. (2020). The mosquito taste system and disease control. Proc. Natl. Acad. Sci. USA *117*, 32848–32856. https://doi.org/10.1073/pnas.2013076117.

44. Dennis, E.J., Goldman, O.V., and Vosshall, L.B. (2019). *Aedes aegypti* mosquitoes use their legs to sense DEET on contact. Curr. Biol. *29*, 1551–1556.e5. https://doi.org/10.1016/j.cub.2019.04.004.

45. Afify, A., Betz, J.F., Riabinina, O., Lahondère, C., and Potter, C.J. (2019). Commonly used insect repellents hide human odors from *Anopheles* mosquitoes. Curr. Biol. *29*, 3669–3680.e5. https://doi.org/10.1016/j.cub.2019.09.007.

46. Hol, F.J., Lambrechts, L., and Prakash, M. (2020). BiteOscope, an open platform to study mosquito biting behavior. Elife *9*, e56829. https://doi.org/10.7554/eLife.56829.

47. Montell, C. (2009). A taste of the *Drosophila* gustatory receptors. Curr. Opin. Neurobiol. *19*, 345–353. https://doi.org/10.1016/j.conb.2009.07.001.

48. Bijma, P. (2011). A general definition of the heritable variation that determines the potential of a population to respond to selection. Genetics *189*, 1347–1359. https://doi.org/10.1534/genetics.111.130617.

49. Hoffmann, A.A., and Merilä, J. (1999). Heritable variation and evolution under favourable and unfavourable conditions. Trends Ecol. Evol. *14*, 96–101. https://doi.org/10.1016/S0169-5347(99)01595-5.

50. Zhao, Z., Zung, J.L., Hinze, A., Kriete, A.L., Iqbal, A., Younger, M.A., Matthews, B.J., Merhof, D., Thiberge, S., Ignell, R., et al. (2022). Mosquito brains encode unique features of human odour to drive host seeking. Nature *605*, 706–712. https://doi.org/10.1038/s41586-022-04675-4.

51. Afify, A., and Potter, C.J. (2022). Genetically encoded calcium indicators for functional imaging of mosquito olfactory neurons. Cold Spring Harb. Protoc. *2022*. pdb.top107683. https://doi.org/10.1101/pdb.top107683.

52. Hammond, A., Galizi, R., Kyrou, K., Simoni, A., Siniscalchi, C., Katsanos, D., Gribble, M., Baker, D., Marois, E., Russell, S., et al. (2016). A CRISPR-Cas9 gene drive system targeting female reproduction in the malaria mosquito vector *Anopheles gambiae*. Nat. Biotechnol. *34*, 78–83. https://doi.org/10.1038/nbt.3439.

53. Konet, D.S., Anderson, J., Piper, J., Akkina, R., Suchman, E., and Carlson, J. (2007). Short-hairpin RNA expressed from polymerase III promoters mediates RNA interference in mosquito cells. Insect Mol. Biol. *16*, 199–206. https://doi.org/10.1111/j.1365-2583.2006.00714.x.

54. Gratz, S.J., Ukken, F.P., Rubinstein, C.D., Thiede, G., Donohue, L.K., Cummings, A.M., and O'Connor-Giles, K.M. (2014). Highly specific and efficient CRISPR/Cas9-catalyzed homology-directed repair in *Drosophila*. Genetics *196*, 961–971. https://doi.org/10.1534/genetics.113.160713.

55. Lobo, N.F., Clayton, J.R., Fraser, M.J., Kafatos, F.C., and Collins, F.H. (2006). High efficiency germ-line transformation of mosquitoes. Nat. Protoc. *1*, 1312–1317. https://doi.org/10.1038/nprot.2006.221.

56. Pondeville, E., Puchot, N., Meredith, J.M., Lynd, A., Vernick, K.D., Lycett, G.J., Eggleston, P., and Bourgouin, C. (2014). Efficient ΦC31 integrase–mediated site-specific germline transformation of *Anopheles gambiae*. Nat. Protoc. *9*, 1698–1712. https://doi.org/10.1038/nprot.2014.117.

57. Volohonsky, G., Terenzi, O., Soichot, J., Naujoks, D.A., Nolan, T., Windbichler, N., Kapps, D., Smidler, A.L., Vittu, A., Costa, G., et al. (2015). Tools for *Anopheles gambiae* transgenesis. G3 *5*, 1151–1163. https://doi.org/10.1534/g3.115.016808.

58. Siju, K.P., Hansson, B.S., and Ignell, R. (2008). Immunocytochemical localization of serotonin in the central and peripheral chemosensory system of mosquitoes. Arthropod Struct. Dev. *37*, 248–259. https://doi.org/10.1016/j.asd.2007.12.001.

59. Poinapen D., Yoshizawa T., Zho Y., Charon N., Mou S., Oshima K., Wood L., Hruban R., Zbijewski W. Three-dimensional Shape and Topology Analysis of Tissue-Cleared Tumor Samples. Proc. SPIE 11603, Medical Imaging 2021: Digital Pathology 1160316. https://doi.org/10.1117/12.2582601.

60. Kramer, J.M., and Staveley, B.E. (2003). GAL4 causes developmental defects and apoptosis when expressed in the developing eye of *Drosophila melanogaster*. Genet. Mol. Res. *2*, 43–47.

61. R Core Team (2022). R: A Language and Environment for Statistical Computing (R Foundation for Statistical Computing).

STAR★METHODS

KEY RESOURCES TABLE

REAGENT or RESOURCE	SOURCE	IDENTIFIER
Antibodies		
rat anti-CD8	Thermo Fisher Scientific	Cat# 14-0081-82; RRID:AB_467087
mouse anti-nc82	DSHB	nc82; RRID: AB_2314866
Cy3 goat-anti rat	Jackson ImmunoResearch	Cat# 112-165-167; RRID: AB_2338251
Alexa-647 goat anti-mouse	Jackson ImmunoResearch	Cat# 115-605-166; RRID:AB_2338914
Bacterial and virus strains		
Stellar Competent Cells	Takara Bio USA	Cat# 636763
Chemicals, peptides, and recombinant proteins		
Phusion DNA Polymerase	New England BioLabs	Cat# M0530L
Millonig's phosphate buffer	Electron Microscopy Sciences	Cat# 1582-05
Triton-X	Electron Microscopy Sciences	Cat# 22140; CAS #9002-93-1
SlowFade Diamond Antifade Mountant	Invitrogen	Cat# S36972
Critical commercial assays		
In-Fusion Cloning Kit	Takara Bio USA, Inc.	Cat# 639645
DNeasy Blood and Tissue Kit	Qiagen	Cat# 69506
ZymoPURE II Plasmid Maxiprep Kit	Zymo Research	Cat# D4203
Experimental models: Organisms/strains		
Anopheles coluzzii: N'Gousso (NGO), wild type	Insect Transformation Facility, Rockville, Maryland	N/A
Anopheles coluzzii: *brp-T2A-QF2^{w}*	This paper	N/A
Anopheles coluzzii: *QUAS-CD8:GFP*	Riabinina et al. 2016[29]	N/A
Anopheles coluzzii: *orco-T2A-QF2 > QUAS-CD8:GFP*	Riabinina et al. 2016[29]	N/A
Oligonucleotides		
gRNA1: AAGCTCTTGAGGAAACCTGCTGG	This paper	N/A
gRNA2: TTTAAGTAAGACCCAGTTATTGG	This paper	N/A
InFusion cloning primer for gRNA (Forward) brp_gRNA_FOR: GTTGCTCTCTGCTTGAAGCTCTTGAGGAAACCTGCGTTTTAGAGCTAGAAATAGCAAGTTA	This paper	N/A
InFusion cloning primer for gRNA (Reverse) brp_gRNA_REV: TTCTAGCTCTAAAACATAACTGGGTCTTACTTAAACAAGCAGAGAGCAACTCC	This paper	N/A
InFusion cloning primer for 5'HA (Forward) brp_5HA_FOR: ATCGTCGAGTGGTACGTGCATTGATTTTGGGTTAGTAATTGCTTGTTTTCTTC	This paper	N/A
InFusion cloning primer for 5'HA (Reverse) brp_5HA_REV: GCCCTCACGCGTTACGAAGAAGCTCTTGAGAAAGCCGGCTGGTC	This paper	N/A
InFusion cloning primer for 3'HA (Forward) brp_3HA_FOR: AATTAGATCTCTCGATGCGACTAGAAACAAAAAACAACTACAAT	This paper	N/A

(*Continued on next page*)

Continued

REAGENT or RESOURCE	SOURCE	IDENTIFIER
InFusion cloning primer for 3'HA (Reverse) brp_3HA_REV: ACGCAGCCGTCTCGAGGTACAAATAGCGATTACACA CTTGCC	This paper	N/A
Primers for genotyping *brp* mosquitoes, see Table S1	This paper	N/A
Recombinant DNA		
Drosophila melanogaster HACK construct	Lin and Potter, 2016[25]; Addgene	#80274
pQUAST-mCD8:GFP	Potter et al. 2010; Addgene[22]	#24351
pXL-BACII-ECFP-15xQUAS-TATA-GCaMP6f-SV40	Afify et al. 2019[45]	N/A
pattB-nsyb-QF2^{w}	Riabinina et al. 2015[24]; Addgene	#46116
pBac-AttB-3xP3-RFP-Vas2-hCas9-U6-BsaI-gRNA-AttB	Hammond et al. 2016[52]	P165 GenBank#: KU189142
Software and algorithms		
Vectorbase	https://vectorbase.org/	N/A
FlyCRISPR	https://flycrispr.org/	N/A
QCapture Pro 7	QImaging	N/A
Fiji ImageJ	https://fiji.sc/	N/A
VolView	https://kitware.github.io/VolView/	N/A
3D Slicer	https://www.slicer.org/	N/A
Imaris	Oxford Instruments	N/A
R	https://www.r-project.org/	N/A
Adobe Illustrator	Adobe, Inc.	N/A
Other		
0.22 Ultrafree MCCentrifugal Filter	Merck Millipore	Cat# UFC30GV0S
BrightStar Plus Nitrocellulose Membrane	Invitrogen	Cat# AM10100
Quarts filaments	Sutter Instruments	Cat# QF100-70-10

RESOURCE AVAILABILITY

Lead contact

Further information and requests for resources and reagents should be directed to and will be fulfilled by the lead contact, Christopher J. Potter (cpotter@jhmi.edu).

Materials availability

Plasmids generated in this study are available from the lead contact upon request.

Data and code availability

- Confocal data files reported in this paper will be shared by the lead contact upon request.
- This paper does not report original code.
- Any additional information required to reanalyze the data reported in this paper is available from the lead contact upon request.

EXPERIMENTAL MODEL AND SUBJECT DETAILS

Mosquito rearing and colony maintenance

Unless otherwise indicated, all wild-type N'Gousso (NGO) and pan-neuronal (brp) *An. coluzzii* mosquitoes were reared at 28±1°C, 80±5 % RH, and 12L:12D light cycle. Eggs were collected on filter paper (Fisherbrand; 9 cm diameter; 09-801B) folded into cones and placed in 3 oz cups filled with reverse osmosis (RO) water. Eggs were hatched into 10 x 12-inch trays (Photoquip Inc. USA) filled with ~ 1L of RO water. Once larvae reached a second instar stage, they were separated and reared at a density of 140-170

individuals/tray until pupation. Larvae were fed daily with ground up TetraMin tropical fish food flakes supplemented with cat food pellets (Cat Chow, Purina) once a week. Collected pupae were allowed to eclose directly into 6 × 6 × 6-inch aluminum cages (BioQuip Products Inc). Adults were supplied with *ad libitum* 10% sucrose solution. Five- to 14-day-old mosquitoes were blood fed on ketamine-anesthetized Swiss Webster mice for 15 minutes or until at least 5-10 females were observed to be fully engorged on blood (as stipulated in Johns Hopkins University animal protocol # MO22M395).

METHOD DETAILS

Plasmid construction and HACK transgenesis

All cloning was performed using In-Fusion Cloning (Clontech #639645) and Stellar Competent cells (Clontech #636763) . Mosquito genomic DNA was extracted using the DNeasy Blood and Tissue Kit (Qiagen #69506). Cloning steps were confirmed by PCR genotyping (Phusion, NEB) and Sanger sequencing (Genewiz).

Construction of Anopheles coluzzii HACK backbone

The *Anopheles coluzzii* HACK backbone was created using the original *Drosophila melanogaster* HACK construct (Addgene #80274)[25] with the following modifications. First, the mosquito HACK backbone was designed to have a negative selection marker (GFP) outside of the knock-in homology arms (see Figure 1C), in addition to the positive selection marker (mCherry) within the sequence to be knocked into the mosquito genome. The negative selection marker is used to ensure that the entire plasmid has not been erroneously inserted at an off-target location in the genome. All correctly HACKed mosquitoes should be mCherry+ and GFP-. The *3XP3-GFP-SV40* negative selection marker cassette was constructed from fragments PCR amplified from *pQUAST-mCD8:GFP* (Addgene #24351) and *pXL-BACII-ECFP-15xQUAS-TATA-GCaMP6f-SV40*.[45] In addition, each of the two separate *Drosophila U6* promoters (*U6-1* and *U6-3*) was replaced with a synthetic gBlock (Integrated DNA Technology) for the *Anopheles gambiae U6* short promoter based on the *AgU6* AnGam-2 sequence from Konet et al.[53] This *Anopheles U6* short promoter was used in tandem to drive expression from each of the two different gRNAs (*AgU6:gRNA1, AgU6:gRNA2*). Finally, piggyBac inverted terminal repeat sequences were included to allow for random integration of the HACK construct into the genome if necessary. We did not use this approach to generate the *brp* knock-in, but random integration in order to establish donor lines for HACKing via genetic cross can be achieved if desired.[26,29]

AgaU6+gRNA core (gBlock) (*U6* promoter is italicized; *BbsI* flanked spacer sequence is lowercase; gRNA scaffold is underlined): CTAGTGATCTGAATTAGATCT*ACGGCTGCGTGTGGCTTCTAACGTTATCCATCG CTAGAAGTGAAACGAGCGTGCGTAGGTATATATATGAAATGGAGTTGCTCTCTGCTT*ggggtcttcgagaa gacctGTTTTAGAGCTAGAAATAGCAAGTTAAAATAAGGCTAGTCCGTTATCAACTTGAAAAAGTGGCA CCGAGTCGGTGCTTTTTTGCCTACCTGGAGCCTGAGAGTTGTTCAATTAATTAATTCTGACGTAAG.

Construction of AcoI QF2$^{brp-HACK}$ and QF2w$^{brp-HACK}$ plasmids

We used the HACK approach to target the gene *bruchpilot* (*brp*) to produce a pan-neuronal *Anopheles coluzzii* knock-in line. The homology arms and gRNAs were designed based on the reference sequence for this gene region from Vectorbase (https://vectorbase.org/; ACON010286), which we checked with sequencing against our lab wild-type NGO strain to adjust for potential SNPs. We selected gRNAs by analyzing the region around the stop codon with https://flycrispr.org/ [54] using the following criteria: one gRNA targeting upstream of the stop codon, the second targeting downstream of the stop codon, the two gRNAs being <100 bp apart, and minimizing predicted off-target cleavage sites. The following gRNAs were selected (PAM sequence in parentheses):

gRNA1 AAGCTCTTGAGGAAACCTGC(TGG)

gRNA2 TTTAAGTAAGACCCAGTTAT(TGG)

Several synonymous nucleotide substitutions were made in the homology arms to prevent these gRNAs from targeting the donor sequence. Homology arms were PCR amplified from genomic DNA, while the gRNAs were amplified from the HACK backbone, with the primers themselves adding in the gRNA sequences in place of the spacer sequence in the backbone. The following primers were used for PCR

amplification and In-Fusion cloning (bold indicates the In-Fusion 15 base pair overhangs, while underline indicates the synonymous base pair substitutions):

brp_gRNA_FOR:

GTTGCTCTCTGCTTGAAGCTCTTGAGGAAACCTGCGTTTTAGAGCTAGAAATAGCAAGTTA

brp_gRNA_REV:

TTCTAGCTCTAAAACATAACTGGGTCTTACTTAAACAAGCAGAGAGCAACTCC

brp_5HA_FOR:

ATCGTCGAGTGGTACGTGCATTGATTTTGGGTTAGTAATTGCTTGTTTTCTTC

brp_5HA_REV:

GCCCTCACGCGTTACGAAGAAGCTCTTGAGAAAGCCGGCTGGTC

brp_3HA_FOR:

AATTAGATCTCTCGATGCGACTAGAAACAAAAAACAACTACAAT

brp_3HA_REV:

ACGCAGCCGTCTCGAGGTACAAATAGCGATTACACACTTGCC

The 5′ homology arm was 1040 base pairs, while the 3′ homology arm was 1075 base pairs. The mosquito HACK backbone was digested with SnaBI to clone in the 5′ homology arm, *XhoI* to clone in the 3′ homology arm, and *BbsI* to clone in the gRNAs.

The original HACK backbone (both for flies and mosquitoes) uses the transcriptional activator QF2. Given the expected broad expression of a pan-neuronal driver, we decided to use *QF2*^{w} which had also been used for a pan-neuronal driver line in *Ae. aegypti*.[27] We therefore replaced the *QF2* sequence with *QF2*^{w} (weak variant) by digesting *AcoI QF2*$^{brp\text{-}HACK}$ with *SfiI* and *AflII*, and subcloning in the PCR amplified *QF2*^{w} sequence from *pattB-nsyb-QF2*^{w} (Addgene #46116).[24]

Knock-in line establishment and verification

Microinjections and knock-in verification

Plasmids for injections were prepared using ZymoPURE II Plasmid Maxiprep Kit (Zymo Research, USA) and eluted in ultrapure water. To create a microinjection mix, *brp-T2A-QF2*^{w} plasmid was mixed with a helper plasmid containing *Cas9* (P165 provided by Andrew Hammond, *pBac[AttB-3xP3-RFP-Vas2-hCas9-U6-BsaI-gRNA-AttB]*; GenBank : KU189142)[52] and 10x microinjection buffer (50mM KCl, 1mM NaPO4, pH 6.8). A total of 500 ng/μL of DNA (1:1 ratio of plasmids, 250 ng/μL each) was used in microinjection buffer (at final concentration of 1x). Prior to injections, the plasmid mix was passed through 0.22 filter (Ultrafree MC Centrifugal Filter, Merck Millipore Ltd; UFC30GV0S).

Microinjections were performed using an adapted method for mosquito germline transformation.[55–57] Briefly, three to four days following blood-feeding, *An. coluzzii* were offered a lid of a 50 mL conical tube filled with a thin layer of RO water, lined with filter paper (Fisherbrand; 3.5 cm diameter; 09-801-BB) and placed in the dark for 15 minutes to allow for oviposition. Using a fine brush (Winstonia Kolinsky Sable Nail-Art Detail Brush #0000), freshly laid eggs were lined up lengthwise against the edge of a cut nitrocellulose membrane (BrightStar Plus; Invitrogen: AM10100) placed on a glass microscope slide with their posterior poles facing up. A piece of cut and moistened filter paper (Fisher Scientific; 09-801B) was laid on top of the membrane to keep the eggs hydrated. Quartz filaments (Sutter Instruments; QF100-70-10) were pulled into injection needles using a P-2000 micropipette puller (Sutter Instruments) with the following parameters: Heat = 700; Vel = 60; Del = 145; Pul = 175. Eggs were injected under an Olympus SZX16

microscope with Olympus SDF PLAPO 1.6xPF lens using FemtoJet and PatchManNP2 (Ependorf North America) micromanipulator. Injection parameters used were: 300-1200 hPa injection pressure (adjusted as needed depending on the opening of the needle), 100-500 hPa back pressure, and 0.1-0.2 s injection time. Injected eggs were kept hydrated and left undisturbed until they were fully melanized, at which point they were transferred to a hatching platform (cut and inverted 25 ml polystyrene reagent reservoir wrapped in paper towel) and placed in a 12.5 × 8.5 × 7 cm plastic container with ~ 120 mL of RO water. A total of 380 eggs were injected and 33 of those hatched.

Surviving adults were separated by sex at pupal stage and crossed *en masse* to NGO individuals of the opposite sex. Crosses were blood-fed 4 times with all progeny screened using an Olympus SZX7 epifluorescence microscope equipped with RFP (for mCherry eye marker) and GFP filters. Animals were illuminated with an X-Cite Series 120Q light source. Images were acquired using a QImaging QIClick Cooled digital CCD camera and QCapture Pro 7 software. In total, 15 G_1 larvae (out of 1364 screened) were positive for the red eye marker (mCherry) and negative for green (GFP) eye marker, indicating that the construct was integrated at the targeted location (HACK conversion rate of 1.1 %). The individual larvae that survived to adult stage were outcrossed to NGO individuals of the opposite sex in 1:3-5 ratio. A single cross from one G_1 female produced viable eggs, making this individual a single founder of the *brp-T2A-QF2*^{w} pan-neuronal line. The knock-in was confirmed by PCR genotyping (Phusion, NEB) using primers that bind outside and inside the brp knock-in region (Figures S1A and S1B and Table S1). The following primers were used to genotype the mosquitoes:

Primer 1F

CTCTCGATGCTATCACTCAGACCAA

Primer 1R

TTCTCAATTGAAGCTAGCAGCAACC

Primer 2F

GCTGAAACAAATGCTTCAGGAAACG

Primer 2R

TGTATTCCGTCGCATTTCTCTC

The amplified fragments were 2037 base pairs and 1831 base pairs from primer set 1 and primer set 2, respectively (Figure S1B).

Reporter expression

Expression was examined by crossing to a *QUAS-mCD8:GFP* reporter line previously established by our lab.[29]

Immunohistochemistry

Brain and ventral nerve cord (VNC) staining was carried out as previously described.[29,58] Briefly, bodies of 9–25 dpe female mosquitoes were fixed in 4% paraformaldehyde in 0.1 M Millonig's phosphate buffered solution (pH 7.4) (Electron Microscopy Sciences: 11582-05) for 3–4 hours at 4°C. Brains and VNCs were dissected out in 1xPBS and washed in PBT (1x PBS containing 0.3% Triton X-100 (Electron Microscopy Sciences: 22140)) for 1 h (3 times, 15-20 min each) at room temperature (RT). The tissues were then permeabilized with a blocking solution (1x PBS containing 4% Triton X-100 and 2% normal goat serum (NGS)) overnight at 4°C. The following day, brains and VNCs were washed for 1h in PBT (3 times, 15-20 min each) at RT and incubated in PBT with 2% NGS with primary antibodies for 3 nights at 4°C. The primary antibodies used were rat anti-CD8 (Invitrogen #MCD0800, 1:100) and mouse anti-nc82 (DSHB, AB_2314866, 1:50). After incubation with primary antibodies, tissues were washed for 1h in PBT (3 times, 15-20 min each) at RT and incubated in PBT with 2% NGS with secondary antibodies for 3 nights at 4°C. The secondary antibodies used were Cy3 goat-anti rat (Jackson ImmunoResearch #112-165-167, 1:200) and Alexa-647 goat

anti-mouse (Jackson ImmunoResearch #115-605-166, 1:200). After incubation in secondary antibodies, brains and VNCs were washed for 1 h in PBT, placed in a mounting solution (*SlowFade* Diamond Antifade Mountant; Invitrogen, S36972) overnight at 4°C, and mounted on microscope slides (Thermo Scientific, 3050-002) the following day. Endogenous CD8:GFP expression in the mounted tissues was visualized using laser confocal microscopy.

Confocal imaging

Female mosquitoes (≥ 7 dpe) were briefly chilled on ice. Individual sensory appendages were removed with a pair of forceps or a fine microblade and mounted on microscope slides in a drop of mounting solution (*SlowFade* Diamond Antifade Mountant; Invitrogen, S36972). Legs were mounted directly after being detached from the bodies. To minimize air bubbles, antennae, palps, and labella were incubated in a fixative solution (4% paraformaldehyde in 0.1 M Millonig's phosphate buffered solution) for 5 minutes prior to being mounted on slides. Imaging of sensory appendages was done within 2 hours of detaching from the body to capture the endogenous GFP signal.

Images of brains, VNCs, and sensory appendages were obtained using a Zeiss LSM 700 confocal microscope equipped with Fluar 10×/0.50 air M27, LCI Plan-Neofluar 25×/0.8 water Korr DIC M27, and Plan-Apochromat 40×/1.3 Oil DIC M27 objectives. Images were acquired at 1024 × 1024-pixel resolution. Images of brains and VNCs were captured with 2.45 μm z-steps using 25x objective. For sensory appendages imaged with 10x and 40x objectives, the z-steps were 2.84 μm and 0.42 μm, respectively. Maximum intensity projections of full z-stacks or partial z-stacks were generated using Fiji/ImageJ (https://fiji.sc/).

Semi-automatic pipeline for 3-D neuron quantification in mosquito appendages

The acquired z-stack raw images for each appendage were processed through a modified image analysis framework[59] in Fiji/ImageJ(v.1.53t), VolView (v.3.4), 3D Slicer (v. 5.0.3), and Imaris (v. 9.9.1) to enable neuron counting in 3D. First, image contrast enhancement was performed using the stack histogram method in ImageJ on the z-stack, followed by image sharpening using unsharp mark filter (radius = 3 px) in ImageJ, and image denoising using the vtkmedian filter (kernel size = 3) in VolView. Masking of the nerve bundle in the images across the entire z-stacks was performed in 3D Slicer. Finally, the spots distribution algorithm in Imaris was used to automatically detect all 3D objects of ~3.5 μm diameter. Each count was adjusted manually to remove detected objects that were not neurons (e.g., brightly labeled sensilla), and neurons that were missed (e.g., overlapping neurons) were added. The adjustments were made in 3D rendered maximum intensity projections and verified in 2-D planes.

Life history and fitness of *brp-T2A-QF2^{w}* mosquitoes

Broad expression of exogenous transcription factor proteins such as GAL4 and QF2 can cause toxicity and lead to behavioral defects and lower fitness in transgenic animals.[24,60] While we used QF2^{w}, a weaker version of QF2,[24] we noticed some defects in the pan-neuronal *brp-T2A-QF2^{w}* individuals after carefully quantifying several life history traits of this line. It is possible that the T2A peptide added to the C-terminus of the Brp protein might also affect its function.

Attempts at making the pan-neuronal line homozygous were not successful, as pan-neuronal male to female crosses produced few, if any, eggs. We thus kept the pan-neuronal line as heterozygotes by crossing the pan-neuronal individuals *en masse* to wild-type counterparts of the opposite sex each generation. Crosses of pan-neuronal males to wild-type females produced a higher number of eggs than crosses of pan-neuronal females to wild-type males. However, the progenies were equally likely to inherit the transgenic copy of the *brp* gene from both males and females, as we did not detect a difference in the proportion of RFP+ larvae between the two pan-neuronal crosses. This trend was consistent over 10 generations. The female-specific defect can be attributed to low host attraction and blood feeding of the heterozygous pan-neuronal females. When kept in small groups with wild-type males, those females were not attracted to a host (anesthetized mouse) and they were thus unable to successfully blood-feed. Only a small proportion of the heterozygous pan-neuronal females successfully blood-fed when kept in large groups of at least 50-100 individuals. Larva to pupa and pupa to adult survival rates of pan-neuronal individuals were comparable to wild-type controls, with only a small increase in time to pupation.

QUANTIFICATION AND STATISTICAL ANALYSIS

Data are reported as means ± standard errors of means (SEM). All statistical analysis was carried out in R v. 4.2.1.[61] All data were checked for normality with QQ plots and Shapiro-Wilk tests. Homogeneity of variance was checked with variance tests (for comparisons between two groups) or with Bartlett tests (for comparisons among more than 2 groups). Number of neurons between genotypes were compared using independent samples t-tests or 1-way ANOVA. For all *orco>CD8:GFP* and *brp>CD8:GFP* antennae, palps, and labella, n = 3. For *brp>CD8:GFP* legs (5th tarsomere), n= 7 (front legs), n= 5 (middle and hind, each). For all statistical comparisons, α was set to 0.05.